ORIGINAL ARTICLE

Tribological study on rapeseed oil with nano-additives in close contact sliding situation

Rajeev Nayan Gupta[1] · A. P. Harsha[1] · Sagar Singh[1]

Abstract

The present work deals with the tribological evaluation of three types of nano-additives, i.e., copper oxide (CuO; $\approx$ 151.2 nm), cerium oxide (CeO$_2$; $\approx$ 80 nm) and polytetrafluoroethylene (PTFE; $\approx$ 90.4 nm) with rapeseed oil under steel–steel sliding contacts. The nano-additives concentrations in the base oil were 0.1, 0.25 and 0.5% w/v for the lubricant formulation. Further, the rapeseed oil was also epoxidized by a chemical method and the tribological behavior was compared with the base oil (unmodified oil) at similar nano-additives concentrations. The ASTM standards were followed for the study of wear preventive and extreme-pressure analysis of nanolubricants, and it was carried out using four-ball tester. In the antiwear test, CeO$_2$ and PTFE nano-additives have shown the significant reduction in the wear scar diameter at the concentration of 0.1% w/v. In the extreme-pressure test, 0.5% w/v concentration was optimum for oxide nanoparticles; however, PTFE nanoparticles did not show positive effect with both the base oils. Different characterization techniques were employed to confirm the oil modification and for the study of the worn surfaces.

Keywords Nano-additive · Epoxidation · Antiwear · Extreme-pressure · Nanolubricant

Introduction

In the recent years, pollution and environment concerns are getting much attention globally as public issues. This is because, a significant proportion of lubricants and their breakdown products lost in the environment pollute our climate directly and indirectly (Nagendramma and Kaul 2012). Primarily, the petroleum products are more hazardous to the environment because of their non-biodegradability at the time. It ruins our eco-system during its whole lifespan from the point of extraction to dump. As per the forecast, the petroleum reserves are limited in numbers and quantity. Therefore, it is necessary to explore sustainable alternatives for the emerging generation (Campanella et al. 2010). In

this prospect, non-toxicity and biodegradability of vegetable oils make them a suitable choice to a petroleum base stock. Along with aforementioned environmental benign properties, vegetable oils have excellent lubricity, desirable viscosity–temperature characteristic and low volatility (Fox and Stachowiak 2007). These are primarily required criteria for the tribology standpoint of view. Vegetable oils also have some shortcomings like inferior low temperature performance (i.e., precipitation, poor flowability at relatively moderate temperature), prone to oxidative degradation, and hydrolytic instability, etc. (Campanella et al. 2010). It can be attenuated with the genetic and chemical modification of vegetable oils with the use of proper additives (Sharma et al. 2006). All vegetable oils have distinct molecular structure, functional group and degree of unsaturation. A higher number of double bonds in the fatty acid chain increase the degree of unsaturation of the vegetable oils, which tends to worsen the tribo-properties (Adhvaryu and Erhan 2002). Double bonds and allylic carbons act as an active site in triglyceride for chemical modification of vegetable oils (Adhvaryu and Erhan 2002). Therefore, modification of vegetable oil through epoxidation process is an essential reaction by which double bond (C=C) changes into oxirane ring, which improves the stability of oil (Abdullah and Salimon

✉ A. P. Harsha
harshaap@gmail.com

Rajeev Nayan Gupta
rajivnayangupta@gmail.com

Sagar Singh
sagarsingh458@gmail.com

1   Department of Mechanical Engineering, Indian Institute of Technology (Banaras Hindu University), Varanasi 221005, India

2010). However, it is influenced by the molar ratio of the reactants, type of catalyst, reaction time and temperature, stirring speed, etc. Notably, different kinds of catalysts (acid and base catalyst, ion exchange resin, enzymes, etc.) have different reaction rates, which influence the percentage conversion/epoxy yield (Abdullah and Salimon 2010; Snežana et al. 2012).

Indeed, vegetable oils alone are not able to provide performance equivalent or better than the mineral/synthetic oils. However, modification of vegetable oil and/or use of additives (i.e., chemical reagent or nanoparticles) may improve the physical properties like thermo-oxidative stability as well as tribo-performances (Sharma et al. 2006; Adhvaryu and Erhan 2002; Abdullah and Salimon 2010; Snežana et al. 2012; Gupta and Harsha 2017a). Also, the fatty acid structure of the vegetable oil plays a critical role in achieving the improved tribological performance (Sui et al. 2016). Recently, nanoparticles are getting much attention to improve the tribo-performance of base oil. In literature, nanoparticle parameters, viz. shape, size, and concentration have been extensively studied with the petroleum-based oil and few with vegetable oils (Gupta and Harsha 2017a; Sui et al. 2016; Dai et al. 2016; Marko et al. 2015). Researchers have also observed a significant improvement in antiwear, antifriction and extreme-pressure properties with the small amount of nanoparticle additives in the base oil (Gao et al. 2002; Lee et al. 2009; Padgurskas et al. 2013; Gupta and Harsha 2017a; Marko et al. 2015; Kalyani et al. 2017; Alves et al. 2013; Dubey et al. 2013; Raina and Anand 2017; Battez et al. 2008).

In view of above, the objective of the investigation was to develop biolubricant by epoxidation process to improve the tribo-properties. In the past, the comparative tribological study of oxide and polymeric nano-additives in rapeseed oil is not reported in the literature. Therefore, three different types of nano-additives, i.e., cerium oxide (CeO_2), copper oxide (CuO) (both ceramic) and polytetrafluoroethylene (PTFE) (polymeric) were used in the rapeseed oil (RO) and epoxidized rapeseed oil (ERO) with different concentrations (0.1, 0.25 and 0.5% w/v) to formulate the nanolubricants and evaluate the antiwear and extreme-pressure (EP) properties. Also, the nano-additive concentration has been optimized for each category and mechanism for improvement in the tribological behavior is discussed.

Experimental

Materials

The rapeseed oil was extracted from moisture-free seeds by expeller pressing method and filtered. The filtered oil was used as the base oil for experimentation. The formic acid (purity 98%) and hydrogen peroxide 30% were procured from Avra chemicals limited, India. Diethyl ether and concentrated sulfuric acid were obtained from Merck India limited. CeO_2, CuO and PTFE nanoparticles were procured from Sigma-Aldrich, United States. Sodium dodecyl sulfate (SDS) was acquired from RICHEM, Shanghai, China. The AISI 52,100 steel balls having 12.7 mm diameter and hardness of 59–61 HRC was used in each experiment.

Methodology

Oil modification

In the present study, formic acid was used as an oxygen carrier, hydrogen peroxide as oxygen donor and sulfuric acid as a catalyst. The opted molar ratio of rapeseed oil:formic acid:hydrogen peroxide was 1:2:20. The measured volume of rapeseed oil was poured into the three-neck round-bottomed flask, and the calculated amount of formic acid added to the flask followed by a small amount of sulfuric acid (2 ml). The temperature and stirring speed, using the magnetic stirrer appended with hot plate (model: C-MAG HS 4 digital, IKA, Germany), was maintained at 55 °C and 600 rpm, respectively. Hydrogen peroxide in the calculated amount added to the solution drop-wise for 30 min. During the addition of hydrogen peroxide, an exothermic reaction takes place and solution temperature shoots up suddenly. Therefore, ice or water bath was used to keep the reaction temperature constant (thermocouple fixed in one of the necks) and a water-jacket reflux condenser was used on the central neck of the flask to avoid evaporation of the solution. After the completion of the reaction, the oil was immediately extracted with diethyl ether and washed with deionized water to remove any free acids using a separating funnel. Finally, the separated oil used as modified oil (i.e., ERO).

Nanolubricant formulation and tribo-testing

Varying concentrations of nano-additives were added in each of the base oils separately and mixed thoroughly with the magnetic stirrer for 30 min and then ultrasonication for 90 min to keep the particles dispersed. A small amount of SDS (0.1 wt%), as a dispersant, was also used in the base oil to change the surface property of nanoparticles. SDS has a combined aliphatic (tail group) and sulfonic acid (head group) structure (Mall et al. 1996; Soomro et al. 2014). Therefore, the addition of SDS in the base oil alters the interaction between the nanoparticles and oil molecules. The typical interaction of the SDS and the oil molecule is presented in Fig. 1. The tail group of SDS interacts with the surface of the nanoparticles and head group with the oil molecules (Ilyas et al. 2017; Gupta and Harsha 2017b). This

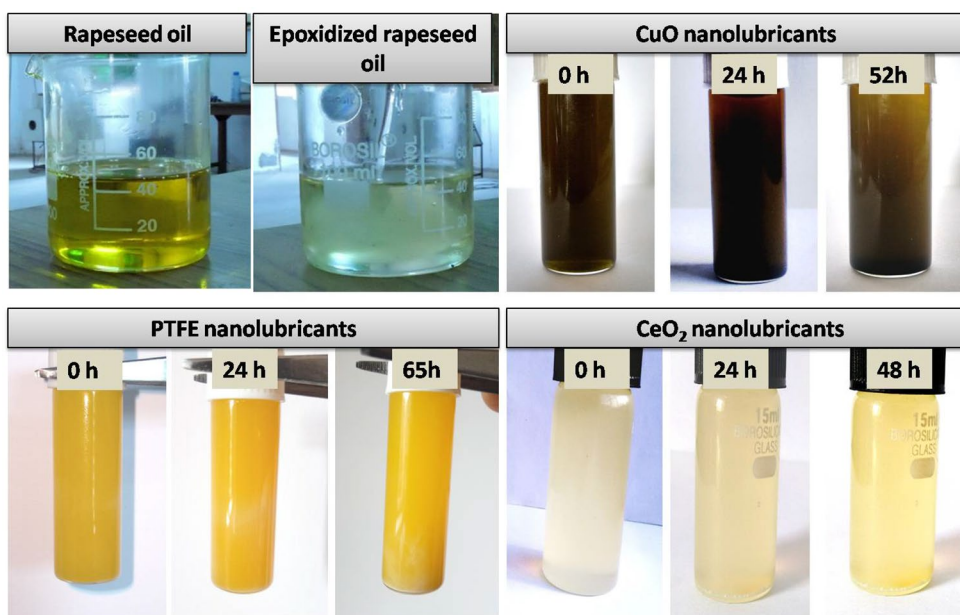Fig. 1 Schematic diagram of nanoparticles in the oil with and without SDS dispersant interaction
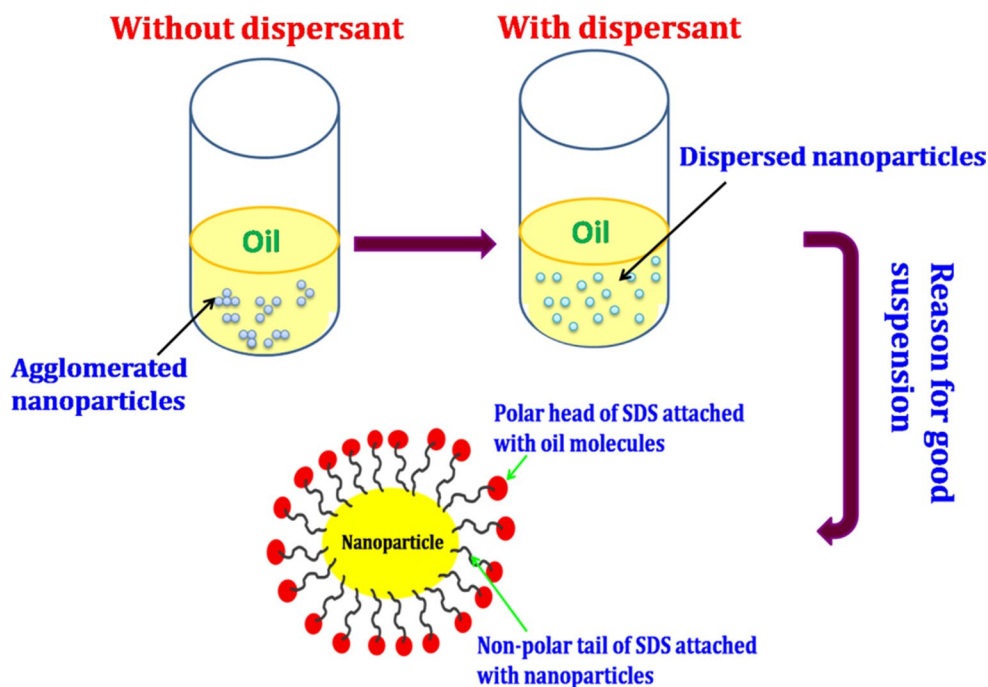

Fig. 2 Typical images of unmodified, epoxidized rapeseed oil, and nanoparticles suspension in the oil

interaction reduces the surface energy of the nanoparticles and helped for the longer suspension.

Antiwear, antifriction and extreme-pressure (EP) behaviors of the formulated oils were examined with four-ball tester as per ASTM standards (D4172 and D2783). The operating parameters for antiwear test were as follows: load 40 kgf (or 392 N), time 1 h, speed 1200 rpm, and temperature 75 °C. And operating condition for EP test were as follows: load was gradually increased from 6 to 800 kgf for

each test, time 10 s, speed 1760 rpm, and room temperature (nearly 27 °C). The detailed test procedure has been reported in our previous study (Gupta and Harsha 2017a). The reproducibility of the test results has been verified by performing each test at least thrice.
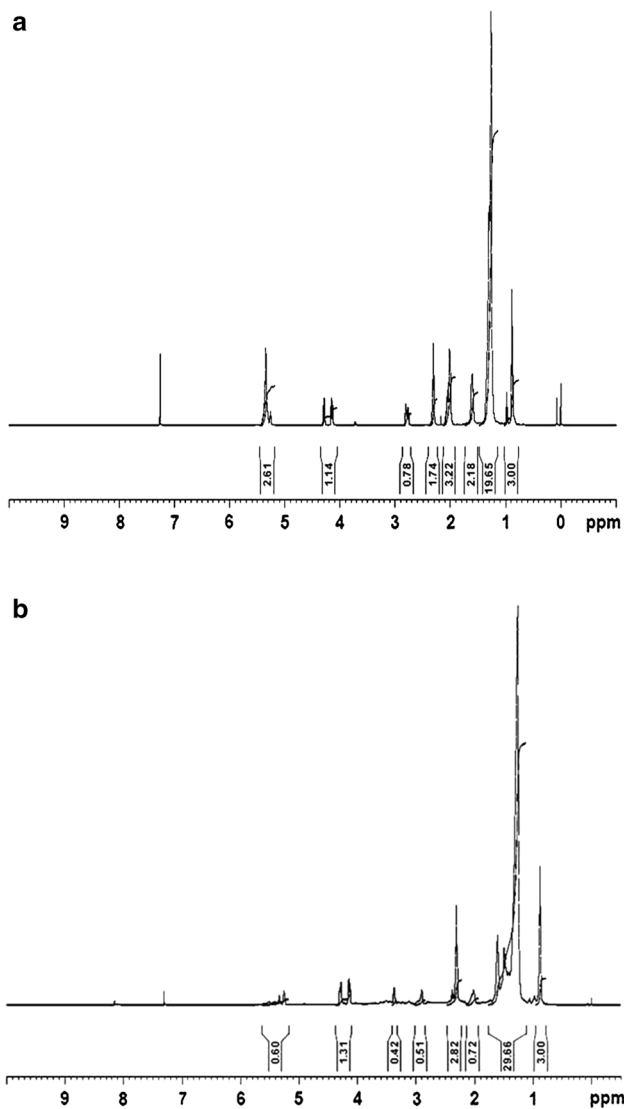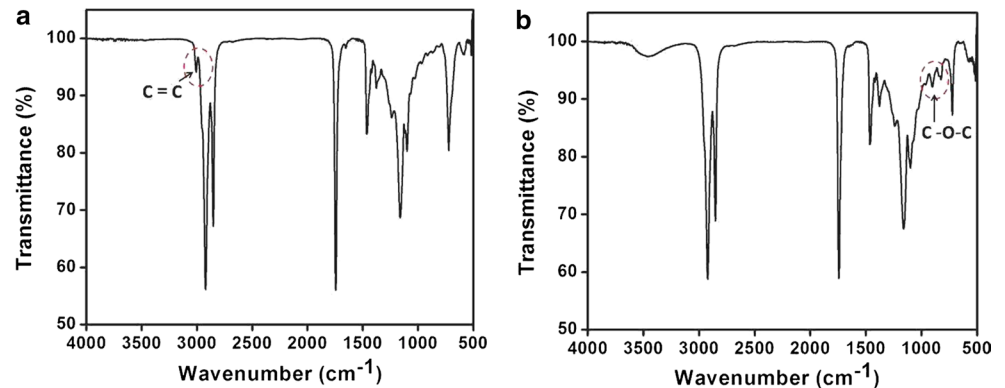
a

b

Fig. 3 Proton NMR for: **a** RO and **b** ERO

Sample characterization

Nuclear magnetic resonance (NMR) spectrometer (model: Bruker 500 AVANCE III HD, Bruker, Rheinstetten, Germany) and Fourier transform infrared (FTIR) spectroscopy (model: Bruker Alpha Eco-ATR, Germany) were used for quantitative analysis of modified and unmodified oil on the basis of presence and absence of proton NMR and absorption peaks, respectively. Iodine value test determined the iodine value of RO and ERO according to AOCS Cd 1–25. Iodine value indicates the degree of saturation of the vegetable oils, which corresponds the thermo-oxidative stability of the vegetable oils. Other analytical tools like scanning electron microscopy (SEM) and energy dispersive spectroscopy (EDS) (model: EVO 18 Research, Zeiss, Germany) were used to examine the shape and size of the nanoparticles as well as for the worn surface analysis of the steel balls. Scanning probe microscopy (SPM) (model: NTEGRA Prima, NT-MDT Spectrum Instruments, Russia) was used to obtain the surface roughness and three-dimensional view of the worn surfaces.

Results and discussion

Oil characterization

The RO is highly susceptible to thermal and oxidation degradation in the presence of olefin and bisallylic proton. The protons related to these carbon atoms are highly reactive and prompt radical-initiated oxidation at these spots due to the existence of oxygen molecules. Hence, to improve the oxidation stability of oil, these reactive protons must be removed. Figure 2 shows the typical image of modified/unmodified rapeseed oil and nanoparticles suspension in the base oil. The oil appearance was changed from dark yellow
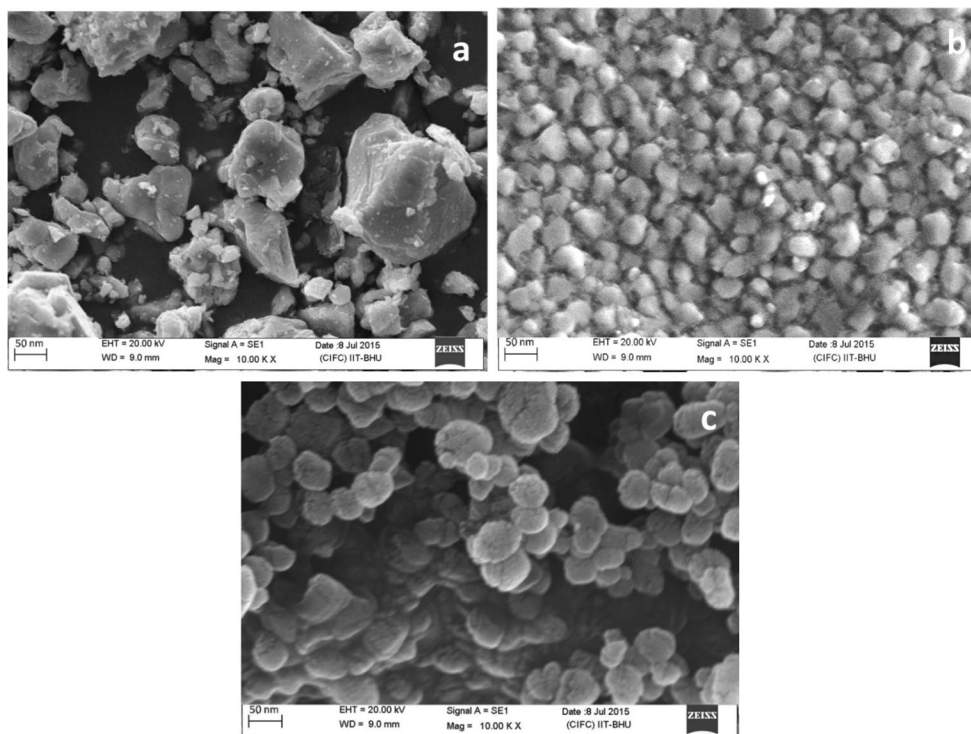
Fig. 4 FTIR spectra for: **a** RO and **b** ERO

⌂ Springer

Fig. 5 SEM image of: **a** CuO, **b** CeO$_2$ and **c** PTFE nanoparticles

Table 1 WSD and COF values for different oil compositions

Type of oil	Raw oil	Nanoparticle concentration (%w/v)								
		CuO			CeO$_2$			PTFE		
		0.1	0.25	0.5	0.1	0.25	0.5	0.1	0.25	0.5
Wear scar diameter (WSD; in μm)										
RO	788.4	710.8	861.4	1052.1	656.6	663.6	736.5	404.0	426.6	682.6
ERO	528.8	804.5	569.1	792.9	485.2	624.8	865.8	700.2	715.0	443.4
Coefficient of friction (COF)										
RO	0.066	0.02	0.026	0.082	0.017	0.046	0.052	0.025	0.027	0.035
ERO	0.029	0.01	0.027	0.061	0.043	0.051	0.052	0.026	0.06	0.061

to pale yellow after epoxidation. In Fig. 2, 0 h represents the nanolubricants just after the ultrasonication. Other abbreviations, i.e., 24, 48, 52, 65 h, were referred according to the elapsed time before settling down of the nano-additives. It is clear that, after 24 h of ultrasonication, all nanoparticles show stable suspension in RO. However, after 52, 65 and 48 h agglomeration of CuO, PTFE and CeO$_2$ nanoparticles were observed. Figure 3a, b shows the proton NMR spectra of RO and ERO, respectively. The relative allocation of CH$_n$ ($n = 0$–3) carbons in the modified and unmodified oils was analyzed. The peak observed due to the proton of the unsaturated carbon (C=C) appears typically at δ 5.2–5.4 ppm, as shown in Fig. 3a. For complete epoxidation reaction, this unsaturation in the rapeseed oil is replaced with the epoxy group at δ 3.1–3.4 (Adhvaryu and Erhan 2002). The epoxy protons are observed in the δ 3.2–3.3 ppm region as in Fig. 3b. Therefore, it can be inferred as epoxidation of RO.

The C=C absorption peak (red circled) was present in the case FTIR of RO at a wavenumber of 3001.8 cm^{-1} (Fig. 4a). This absorption peak completely disappeared in ERO, as can be seen in Fig. 4b and new absorption peak has appeared at 827 cm^{-1}. This is the precise evidence of completion of epoxidation reaction and formation of the C–O–C bond. Also, this indicates the formation of oxirane ring and C–O stretching of the ring in a range of 820–843 cm^{-1} (Salih et al. 2011). A broad absorption peak was also observed at 3470 cm^{-1}, which indicates OH stretch of hydroxyl group for ERO.
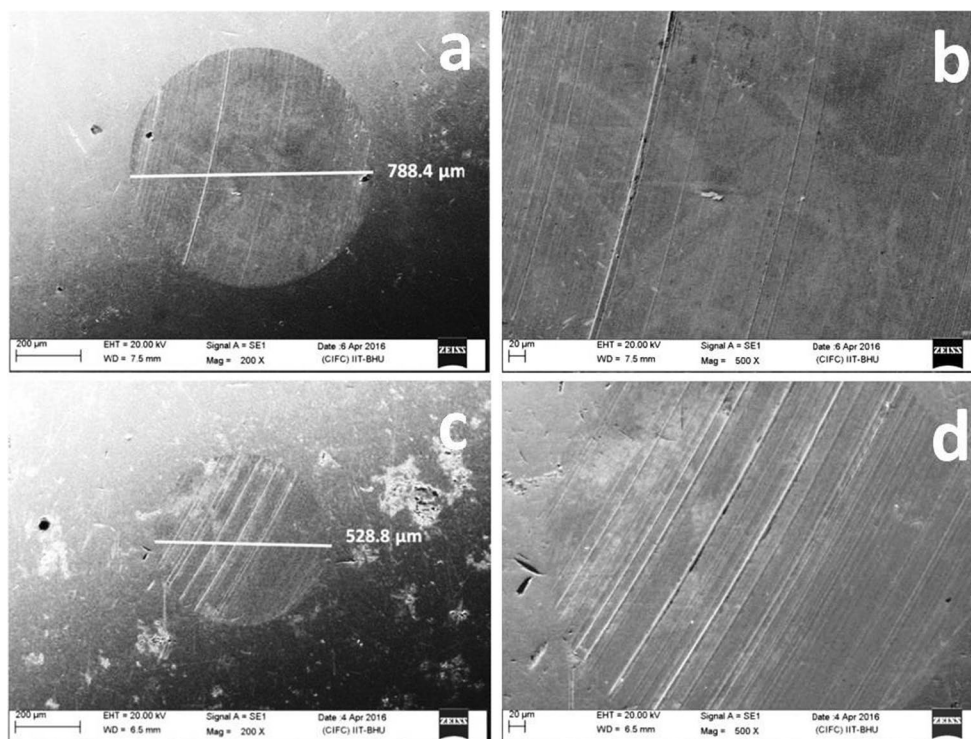
Fig. 6 Worn surfaces of steel balls tested with: **a**, **b** RO and **c**, **d** ERO; at load 392 N, temperature 75 °C for 1 h (**b**, **d** at 500×)
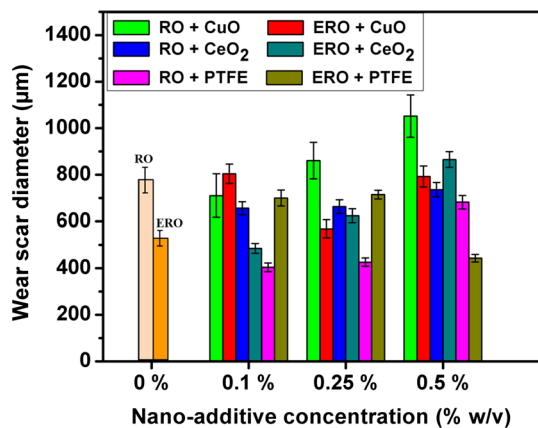

Fig. 7 Variations of WSD with different nano-additive concentrations in the oils

The iodine value of the vegetable oil is an indicator of the presence of the amount of fatty acids with double bonds. The obtained iodine values for the RO and ERO were 96 and 6, respectively. The low iodine value of vegetable oil has a high degree of saturation and vice versa. It can also be linked with the thermo-oxidative stability of the rapeseed oil, i.e., modified oil has good stability as compared to the unmodified oil.

Nanoparticle characterization

The size and morphology of the CuO, CeO$_2$ and PTFE particles are shown in Fig. 5. It was observed that the shape of CeO$_2$ and PTFE nanoparticles are almost spherical. However, CuO nanoparticles have a combination of spherical and irregular shape. The size variations of nanoparticles are reported by measuring a hundred particles with IMAGE J software. The estimated average size of CuO, CeO$_2$ and PTFE particles was observed to be 151.2, 80 and 90.4 nm, respectively.

Wear performance

For pure base oils

Table 1 enumerates the wear scar diameter (WSD) and friction coefficient for different compositions of oils. Figure 6 shows the wear scar on the steel balls tested with RO and ERO (without additive) at different magnifications. The observed WSD was 788.4 μm for RO; however, it reduced to 528.8 μm for ERO. The variations in WSD size for the base RO and ERO were 5.6 and 4.3%, respectively (for three repeated tests). The reduction in the WSD by 33% for
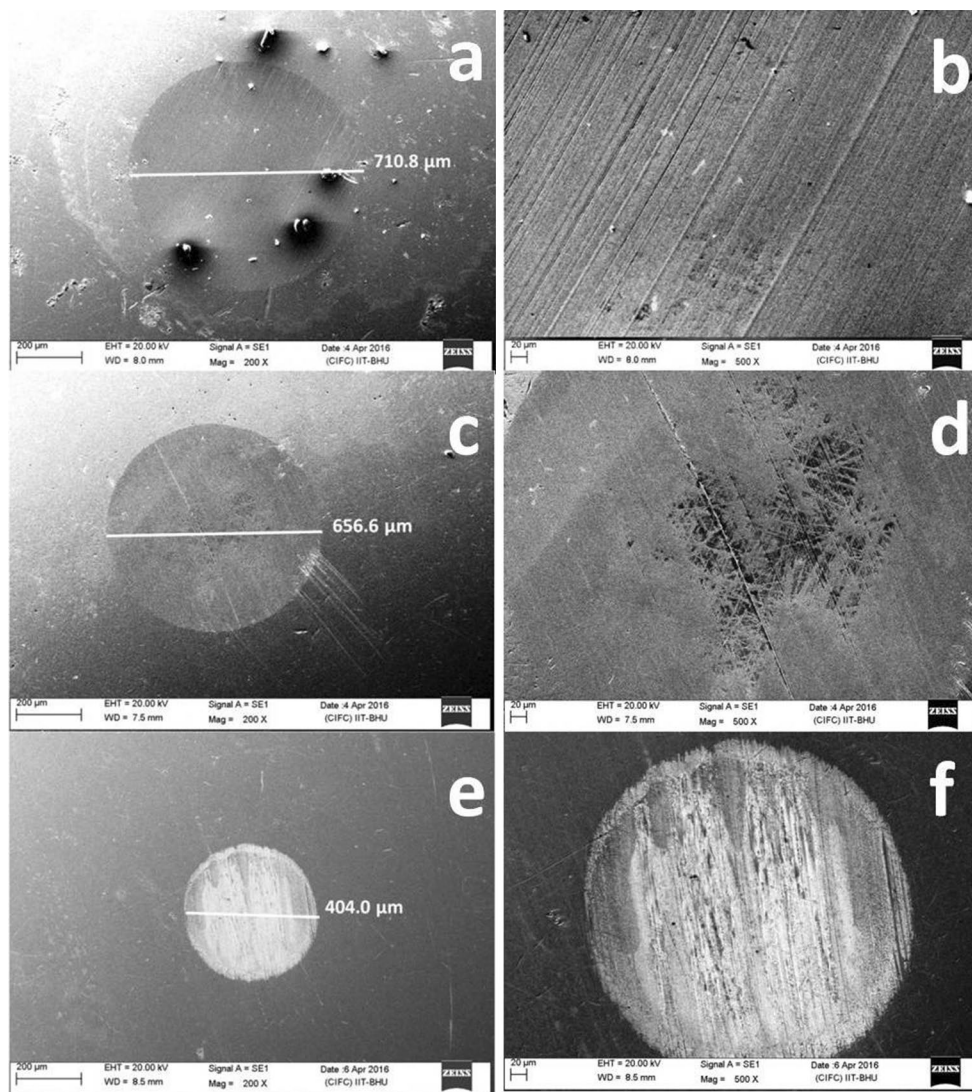
Fig. 8 Worn surfaces of steel balls tested with nanolubricants at optimum concentration of: **a**, **b** CuO; **c**, **d** CeO$_2$ and **e**, **f** PTFE nanoparticles in RO; at load 392 N, temperature 75 °C for 1 h (**b**, **d** and **f** at 500×)

modified oil ascribes the presence of the functional group in the fatty acid structure. These functional groups maintain the adherence ability and lubricity of oil by strong physisorption and chemisorptions at the mating surfaces, which directly helps in the wear reduction (Arumuam and Sriram 2013). At higher magnification, the appearance of the worn track of the ball lubricated with RO revealed fine scratches while ERO shows shallow grooves. It may be due to better tribofilm formation in the presence of polar group to separate metal–metal contact.

For nano-additive-based oils

Figure 7 depicts the WSD variations for all the nanolubricant compositions of RO and ERO. It shows the variation range of the wear size is higher for the CuO-based nanolubricants as compared to the CeO$_2$ and PTFE nanolubricants. This deviation was even higher than base oil also. The SEM images of wear scar for different nano-additive compositions with RO and ERO are depicted in Figs. 8 and 9, respectively. The obtained deep and shallow grooves, scratches, transfer film, etc., indicate the close contact situation as well as boundary lubrication regime (Ghaednia et al. 2015a). In the case of CuO nano-additive in both the base oils, no reduction in WSD was obtained, except for the concentration of 0.1% w/v in RO (Table 1). It reflects that CuO nanoparticles were not compatible either with unmodified or modified rapeseed oil. On the contrary, a remarkable reduction in the WSD was observed with CeO$_2$ and PTFE nanoparticles. It speculated that the morphology along with the concentration of the nanoparticles might be responsible for such behavior. In tribological contact situations, the nano-additives having a
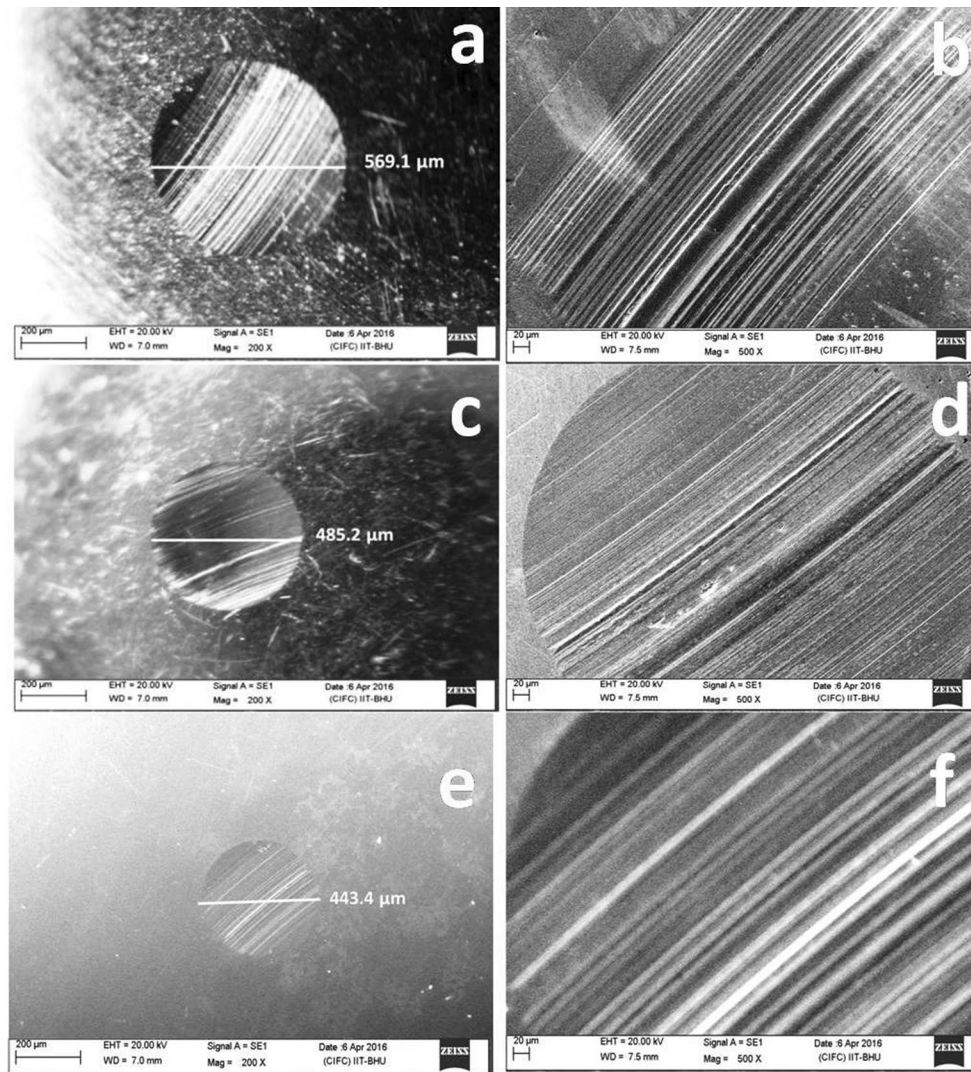
Fig. 9 The lowest WSD observed in nanolubricants with **a, b** CuO; **c, d** CeO$_2$ and **e, f** PTFE nanoparticles in ERO; at load 392 N, temperature 75 °C for 1 h (**b, d** and **f** at 500×)

Fig. 10 Variations in: **a** mean wear volume and **b** interfacial shear stress for different oil compositions (note: interfacial shear stress = COF × material flow stress)
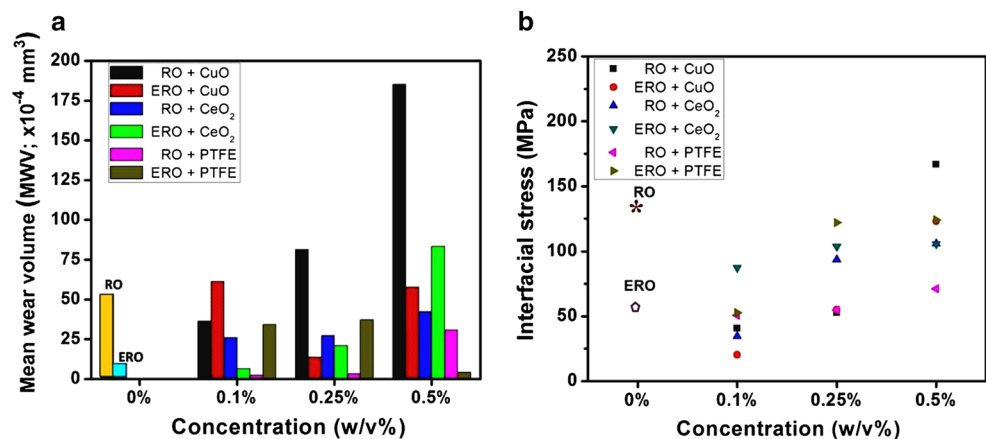
Table 2 Interfacial shear stress values for different oil compositions

Type of oil	Raw oil	Nanoparticle concentration (%w/v)								
		CuO			CeO$_2$			PTFE		
		0.1	0.25	0.5	0.1	0.25	0.5	0.1	0.25	0.5
Interfacial shear stress* (MPa)										
RO	134.6	40.68	52.8	166.7	34.57	93.56	106	50.85	54.9	71.2
ERO	58.98	20.3	55	124.07	87.4	103.7	105.7	52.8	122	124.1

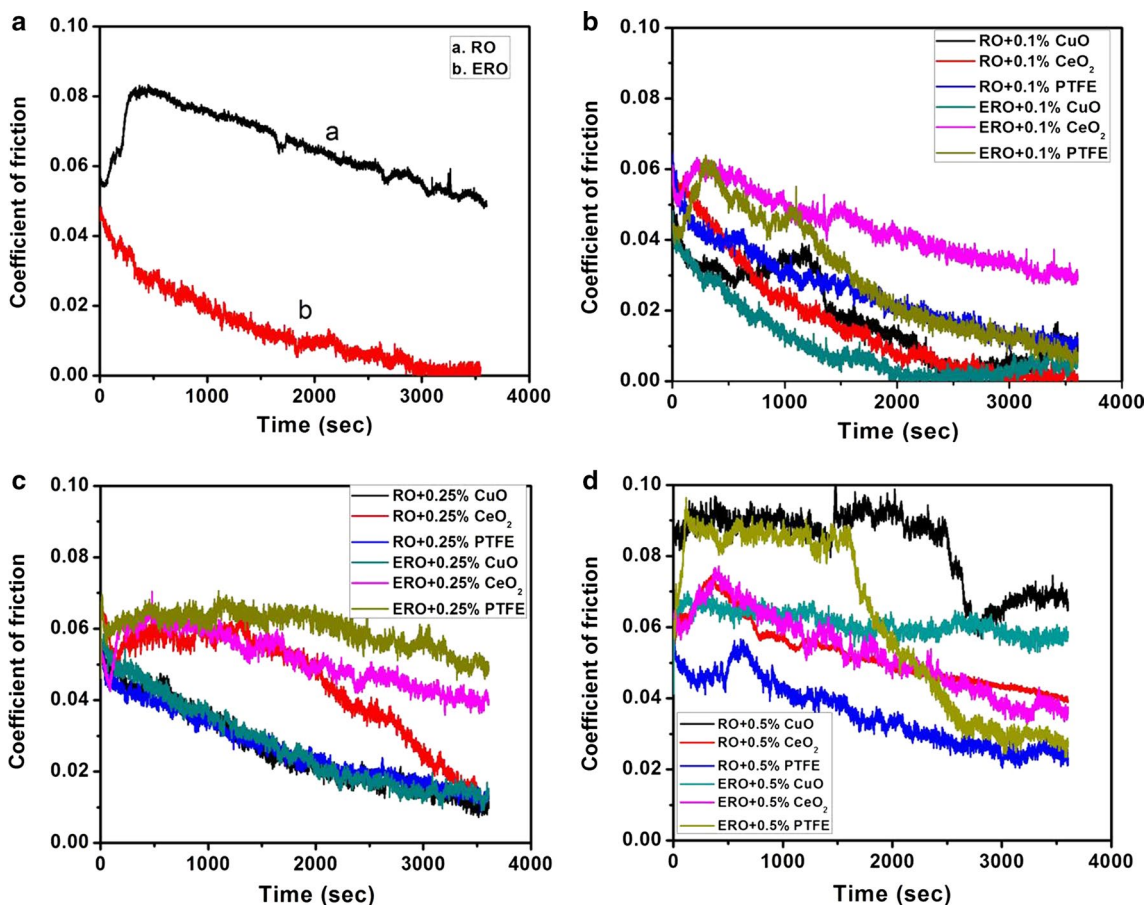*Interfacial shear stress $(\tau_i) = \text{COF} \times$ flow stress of material

Fig. 11 Variations in coefficient of friction with: **a** base oils without additive, **b** 0.1% w/v, **c** 0.25% w/v and **d** 0.5% w/v of nano-additives in the base oils tested at 392 N load for 1 h

lower aspect ratio (the ratio of major to minor dimension) like spherical shape could perform better than the higher aspect ratio (Hwang et al. 2011; Dai et al. 2016; Hu et al. 2010). In this study, the CeO$_2$ and PTFE nanoparticles are almost spherical (Fig. 5), thus better tribo-performance. In the case of CeO$_2$ nano-additive in both base oils, the maximum reduction in WSD was 16.7 and 8.2% at a concentration of 0.1% w/v as compared to RO and ERO, respectively. Although, PTFE is a well-known material for lowering the friction, nevertheless, PTFE nanoparticle as a lubricant

additive elucidates benchmarking antiwear performance in our study. At the lowest concentration, the WSD was reduced by 48.7% as compared to the RO. Also, at 0.5% w/v concentration of PTFE in ERO has also reduced the WSD by 16.1%. It shows the good compatibility of PTFE nanoparticles with rapeseed oil.

The variations in mean wear volume (MWV) of steel balls and interfacial shear stress between the mating surfaces for all compositions are presented in Fig. 10. The trend of MWV variation is approximately similar to the WSD because the

Table 3 EP behavior of different oil compositions

Oil composition	CuO		CeO$_2$		PTFE	
Additive concentration (%w/v)	Last non-seizure load (kgf)	Weld load (kgf)	Last non-seizure load (kgf)	Weld load (kgf)	Last non-seizure load (kgf)	Weld load (kgf)
RO (0%)	126	160	126	160	126	160
ERO (0%)	126	160	126	160		
RO+ 0.1%	126	160	126	160		
RO+ 0.25%	126	160	160	200		
RO+ 0.5%	160	200	160	200		
ERO+ 0.1%	126	160	126	160		
ERO+ 0.25%	126	160	126	160		
ERO+ 0.5%	160	200	160	200		

MWV is calculated from the mean WSD. Table 2 represents the summary of shear stress at the interface. RO has the higher interfacial stress of 134.6 MPa compared to ERO (i.e., 58.98 MPa). For nano-additive-based oil compositions, the variation of the interfacial stress is similar to the friction behavior. This is because, the shear stress at the interface is calculated with the help of coefficient of friction (COF), and it is in direct proportion.

Mechanism for antiwear

In the case of CeO$_2$ in RO and ERO, 0.1% w/v was optimum concentration because of the lowest WSD. It indicates that the optimum number of particles were available even after squeezing out of nanolubricant under high contact stress (Gupta and Harsha 2017a). Also, a uniformly suspended CeO$_2$ nanoparticle separates the asperity–asperity contact at this lower concentration. It is also proposed that the in situ secondary tiny particles may generate by shearing the top layer of the nanoparticles under higher contact stress during sliding (Wäsche et al. 2015). These secondary particles (wear debris and/or nanoparticles) fill the surface dimples and nano-grooves of the mating surfaces. Also, the real area of contact was also reduced by the nanoparticles to achieve lower wear rate (Ghaednia and Jackson 2013b). In spite of this, somewhere adhesive wear was prominent that caused transfer layer on the ball in few areas as shown in Fig. 8d. However, beyond the optimum concentration, with the increase in CeO$_2$ concentration in both the base oils, the WSD continuously increased. It was due to third body abrasion of ball material with harder nanoparticles, and this revealed as plowing marks (Fig. 9).

On the other hand, PTFE in RO and ERO have shown incisive tribo-results at the concentration of 0.1 and 0.5% w/v, respectively. Probably, at higher contact stress and due to the localized frictional heat generated during sliding, PTFE gets activation energy (Barry et al. 2015). It causes PTFE chain fragmentation by breaking –C–C– and/or –C–F– bonds (Biswas and Kalyani 1992; Jintang and Hongxin 1988). These fragmented PTFE react with oxides on a metal surface or atmospheric oxygen, and forms peroxide radicals (Jintang and Hongxin 1988). The oxygen containing radicals have strong polarity to bind PTFE molecules with mating surfaces, thus strong adhesion (Biswas and Kalyani 1992). It results in the formation of a mono- or multi-layer film on the mating surfaces. These layers are elastically deformed and keep the bulk surfaces separated during asperity–asperity contact, thus wear minimized.

Friction performance

The friction behavior of RO and ERO with different nano-additives compositions is presented in Fig. 11. During the initial few minutes of the test, a remarkable increase in friction coefficient was observed, and then continuously decreases to the asymptotic value at the end of the test. The rise in COF indicates the running-in period. It can also infer that initially reaction film not formed on the mating surfaces. Also, the mean COF (for RO) was higher than that of ERO as in Fig. 11a. This was probably due to the oxirane ring formed after the epoxidation process that has improved the lubricity and adhesive property of the base oil.

Alves et al. (2013) studied the compatibility of nanoparticle with the base oil which influences on the tribo-capacity of nanolubricant. Figure 11b, c, d illustrates the variation in COF for oils with 0.1, 0.25 and 0.5% w/v nano-additives, respectively. The four observations made from the obtained results; first, the mean COF (Table 1) were increased with increase in the concentration for all the additives. Second, the lower concentration was sufficient to achieve the minimum friction coefficient for CuO nano-additive in both RO and ERO. Third, for all the concentrations of CeO$_2$ in RO the COF was improved; in contrast, the friction property impaired with ERO irrespective of the concentration. Fourth, the good compatibility of PTFE found with RO at all
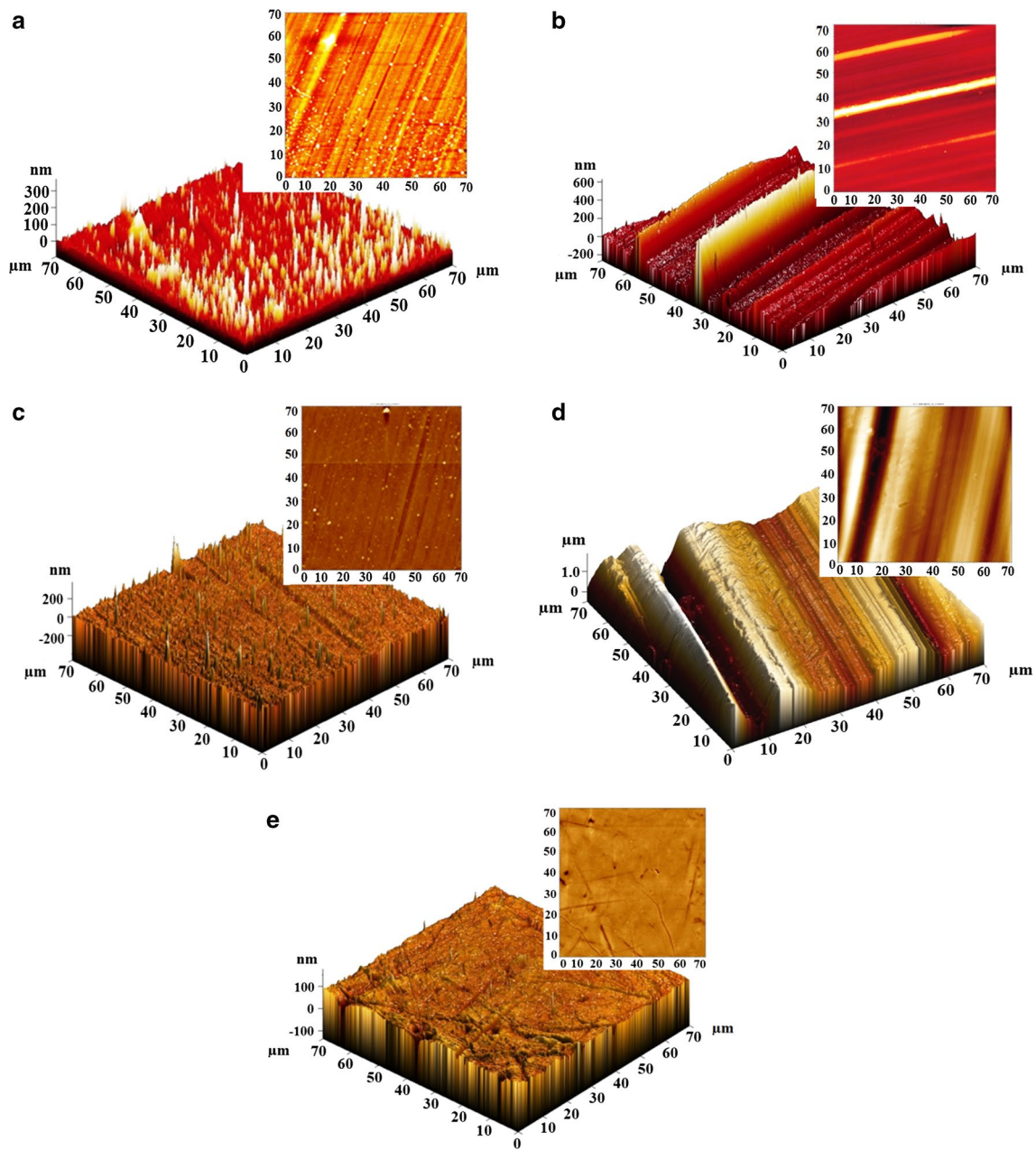
Fig. 12 SPM roughness images of worn surfaces of steel balls tested with: **a** RO, **b** ERO, **c** RO with CeO$_2$, **d** ERO with CeO$_2$ and **e** RO with PTFE nanoparticles (load 392 N, temperature 75 °C for 1 h)

the concentrations; however, modified oil has shown remarkable improvement in antifriction results only at 0.1% w/v.

Mechanism of antifriction

The CuO and CeO$_2$ nanoparticles in RO at lower concentrations have low friction values as compared to the base oil due to an optimum number of particles to separate the asperities. With the increase in the concentration, particles come closer to each other that restrict Brownian motion of the nanoparticles and tend to agglomerate (Wei and Huaqing 2012). It may start to act as an abrasive agent. Also, particles at the mating interface reduce the real area of contact and rolling-sliding of particles takes place. It reduces the friction coefficient for the oxide particles. When PTFE particles are entrapped between the mating surfaces the PTFE chain undergoes scission, which forms an active group that chemically reacts with the contacting surfaces (Harris et al. 2015). This evolves strong adhesion and coherent transfer film (Biswas and Kalyani 1992). Then further interaction between the
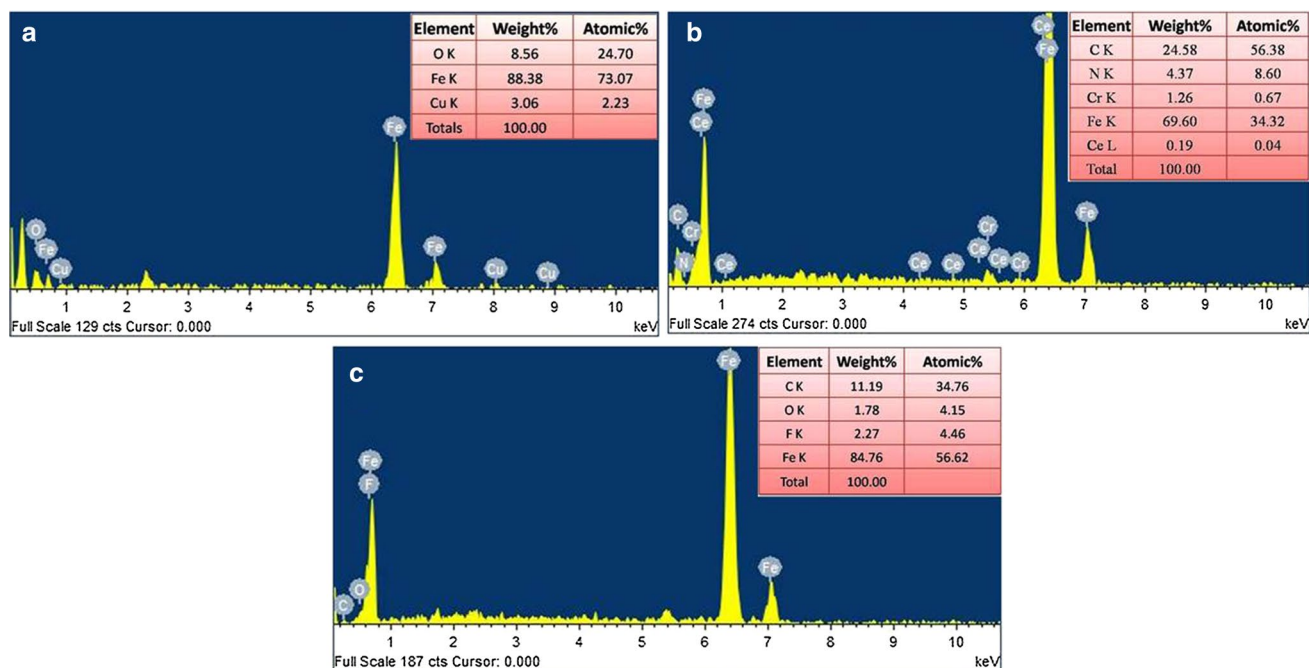
a

Element	Weight%	Atomic%
O K	8.56	24.70
Fe K	88.38	73.07
Cu K	3.06	2.23
Totals	100.00	

b

Element	Weight%	Atomic%
C K	24.58	56.38
N K	4.37	8.60
Cr K	1.26	0.67
Fe K	69.60	34.32
Ce L	0.19	0.04
Total	100.00	

c

Element	Weight%	Atomic%
C K	11.19	34.76
O K	1.78	4.15
F K	2.27	4.46
Fe K	84.76	56.62
Total	100.00	

Fig. 13 Typical EDS image of worn track of steel balls tested with different nanoparticles in ERO: **a** CuO, **b** CeO$_2$ and **c** PTFE at optimum concentration

adhered PTFE on the metallic surface and polymer particles give rise to anisotropic deformation, which results in the closeness of adjacent chains (Jang et al. 2007). It helps in smooth shear of the chain and reduction in friction (Jang et al. 2007; Biswas and Kalyani 1992).

Extreme-pressure performance

Table 3 enumerates the last non-seizure load and weld load capacity of the oil. Weld load performance of the ERO, without additive, was similar to RO. The lower concentrations of oxide particles did not show any significant improvement in the weld load performance, except for 0.5% w/v, for both RO and ERO. Although, 0.25% w/v CeO$_2$ in RO has shown improvement in the weld load in few repeated tests, while not such improvement with ERO. Laura et al. (2014) also observed such trend in load carrying capacity of four different nanofluids used in deep drawing, stamping, and metal working process. Further, no improvement with the addition of PTFE in RO and ERO was observed at any concentration. The maximum improvement in weld load noticed as 200 kgf at 0.5% w/v concentration of CuO and CeO$_2$ in both RO and ERO, while 160 kgf for rest of the concentrations. The reason for such improvement may be due to the variation in the size of the nanoparticles. Lovell et al. (2010) argued that the smaller size nanoparticles smoothen the surface by filling

the dimples, whereas bigger size nanoparticles separate the mating surfaces and support the load.

Surface roughness and elemental analysis of worn surface

Figure 12 illustrates the three-dimensional roughness image of the lubricated worn surfaces with different concentrations. Figure 12a, c, and e shows the roughness image of worn surface lubricated with RO, RO with 0.1% w/v CeO$_2$ and RO with 0.1% w/v PTFE, respectively, having the corresponding r.m.s. area roughness values (S_q) 32, 26 and 25 nm. However, higher roughness values obtained with ERO compositions. Figure 12b, d represents the roughness image of ERO and ERO with CeO$_2$-lubricated surface, having the corresponding roughness (S_q) of 107 and 806 nm, respectively. The aforementioned results reveal that good synergy of nano-additives with RO than ERO.

The typical elemental analysis of the worn surface lubricated with CuO, CeO$_2$, and PTFE nano-additives in the base oils is presented in Fig. 13. Few worn surfaces have shown the traces of the nanoparticle along with the significant iron content. It may be due to the entrapment of the broken hard and brittle oxide particles in a comparative softer ball or strong adhesion of PTFE particles with the mating surfaces. Thus, the presence of oxygen on the worn surfaces may be due to the additive.

Conclusions

The following conclusions are drawn from the present investigation:

1. The RO was successfully epoxidized, and it was confirmed through NMR, FTIR and iodine value tests. The iodine value test result indicates the improvement in the thermo-oxidative stability of the ERO.

2. CuO as an additive in the ERO and RO impairs the antiwear property at all the concentrations. However, CeO_2 and PTFE nano-additives have shown remarkable improvement in the antiwear property for RO with 0.1% w/v concentration, and begin to deteriorate the property with an increase in the concentration.

3. The friction coefficient improved at all the concentrations of CuO, CeO_2, and PTFE nano-additives in RO, therefore 0.1% w/v was assumed to be optimum in the tested range. Also, 0.1% w/v of CuO and PTFE was optimum in ERO, whereas CeO_2 did not show any such improvement in COF.

4. For CuO nano-additive in both oils, weld load capacity improved at 0.5% w/v concentration (i.e., 200 kgf). However, for CeO_2 in RO and ERO the weld load capacity was improved at 0.25 and 0.5% w/v concentration, respectively. The presence of PTFE has not shown any effect on the weld load. For all PTFE concentrations, the weld load was same as base oil.

References

Abdullah BM, Salimon J (2010) Epoxidation of vegetable oils and fatty acids: catalysts, method and advantages. J Appl Sci 10(15):1545–1553

Adhvaryu A, Erhan SZ (2002) Epoxidized soybean oil as a potential source of high temperature lubricants. Ind Crops Prod 15(3):247–254

Alves SM, Barros BS, Trajano MF, Ribeiro KSB, Moura E (2013) Tribological behavior of vegetable oil-based lubricants with nanoparticles of oxides in boundary lubrication conditions. Tribol Int 65:28–36

Arumuam S, Sriram G (2013) Preliminary study of nano- and microscale TiO_2 additives on the tribological behavior of chemically modified rapeseed oil. Tribol Trans 56(5):797–805

ASTM D2783 (Reapproved 2009) Standard test method for measurement of extreme-pressure properties of lubricating fluids (Four-ball method). ASTM International, 100 Barr Harbor Drive, PO Box C700, West Conshohocken, PA 19428-2959, United States

ASTM D4172 (Reapproved 2010) Standard test method for wear preventive characteristics of Lubricating fluid (four-ball method). ASTM International, 100 Barr Harbor Drive, PO Box C700, West Conshohocken, PA 19428-2959, United States

Barry PR, Chiu PY, Perry SS, Sawyer WG, Sinnott SB, Phillpot SR (2015) Effect of temperature on the friction and wear of PTFE by atomic-level simulation. Tribol Lett 58(50):1–13

Battez AH, González R, Viesca JL, Fernández JE, Fernández JMD, Machado A, Chou R, Riba J (2008) CuO, ZrO_2 and ZnO nanoparticles as antiwear additive in oil lubricants. Wear 265:422–428

Biswas SK, Kalyani V (1992) Friction and wear of PTFE—a review. Wear 158:193–211

Campanella A, Rustoy E, Baldessari A, Baltanás MA (2010) Lubricants from chemically modified vegetable oils. Bioresour Technol 101(1):245–254

Dai W, Kheireddin B, Gao H, Liang H (2016) Role of nanoparticles in oil lubrication. Tribol Int 102:88–98

Dubey MK, Bijwe J, Ramakumar SSV (2013) PTFE based nano-lubricants. Wear 306:80–88

Fox NJ, Stachowiak GW (2007) Vegetable oil-based lubricants—a review of oxidation. Tribol Int 40(7):1035–1046

Gao Y, Chen G, Oli Y, Zhang Z, Xue Q (2002) Study on tribological properties of oleic acid-modified TiO_2 nanoparticle in water. Wear 252(5–6):454–458

Ghaednia H, Jackson RL (2013) The effect of nanoparticles on the real area of contact, friction, and wear. J Tribol 135(4):041603

Ghaednia H, Jackson RL, Khodadadi JM (2015) Experimental analysis of stable CuO nanoparticle enhanced lubricants. J Exp Nanosci 10(1):1–18

Gupta RN, Harsha AP (2017a) Synthesis, characterization, and tribological studies of calcium–copper–titanate nanoparticles as a biolubricant additive. J Tribol 139(2):021801

Gupta RN, Harsha AP (2017b) Antiwear and extreme pressure performance of castor oil with nano-additives. Proc IMechE Part J. https://doi.org/10.1177/1350650117739159

Harris KL, Pitenis AA, Sawyer WG, Krick BA, Blackman GS, Kasprzak DJ, Junk CP (2015) PTFE tribology and the role of mechanochemistry in the development of protective surface films. Macromolecules 48(11):3739–3745

Hu KH, Hu XG, Xu YF, Huang F, Liu JS (2010) The effect of morphology on the tribological properties of MoS_2 in liquid paraffin. Tribol Lett 40:155–165

Hwang Y, Lee C, Choi Y, Cheong S, Kim D, Lee K, Lee J, Kim SH (2011) Effect of the size and morphology of particles dispersed in nano-oil on friction performance between rotating discs. J Mech Sci Technol 25(11):2853–2857

Ilyas SU, Pendyala R, Marneni N (2017) Stability of nanofluids (Chapter 1), engineering applications of nanotechnology: from energy to drug delivery. In: Topics in mining, metallurgy and materials engineering. Springer, Cham, pp 1–31. https://doi.org/10.1007/978-3-319-29761-3

Jang I, Burris DL, Dickrell PL, Barry PR, Santos C, Perry SS, Phillpot SR, Sinnott SB, Sawyer WG (2007) Sliding orientation effects on the tribological properties of polytetrafluoroethylene. J Appl Phys 102:123509

Jintang G, Hongxin D (1988) Molecule structure variations in friction of stainless steel/PTFE and its composite. J Appl Polym Sci 36(1):73–85

Kalyani JV, Rastogi RB, Kumar D (2017) The investigation of different particle size magnesium-doped zinc oxide ($Zn_{0.92}Mg_{0.08}O$) nanoparticles on the lubrication behavior of paraffin oil. Appl Nanosci 7:275–281

Laura P-P, Jaime T-T, Andrés G, Demófilo M, Jesús AG, David M, Eduardo P, Pablo C (2014) Antiwear and extreme pressure properties of nanofluids for industrial applications. Tribol Trans 57(6):1072–1076

Lee C-G, Hwang Y-J, Choi Y-M, Lee J-K, Choi C, Oh J-M (2009) Tribological study on the tribological characteristics of graphite nanolubricants. Int J Precis Eng Manuf 10(1):85–90

Lovell MR, Kabir MA, Menezes PL, Higgs CF III (2010) Influence of boric acid additive size on green lubricant performance. Philos Trans R Soc A 368:4851–4868

Mall S, Buckton G, Rawlins DA (1996) Dissolution behaviour of sulphonamides into sodium dodecyl sulfate micelles: a thermodynamic approach. J Pharm Sci 85(1):75–78

Marko M, Kyle J, Branson B, Terrell E (2015) Tribological improvements of dispersed nanodiamond additives in lubricating mineral oil. J Tribol 137:011802

Nagendramma P, Kaul S (2012) Development of ecofriendly/biodegradable lubricant: an overview. Renew Sustain Energy Rev 16(1):764–774

Padgurskas J, Rukuiza R, Prosyčevas I, Kreivaitis R (2013) Tribological properties of lubricant additives of Fe, Cu and Co nanoparticles. Tribol Int 60:224–232

Raina A, Anand A (2017) Tribological investigation of diamond nanoparticles for steel/steel contacts in boundary lubrication regime. Appl Nanosci 7:371–388

Salih N, Salimon J, Yousif E (2011) The physicochemical and tribological properties of oleic acid based trimester biolubricants. Ind Crops Prod 34:1089–1096

Sharma BK, Adhvaryu A, Liu Z, Erhan SZ (2006) Chemical modification of vegetable oils for lubricant applications. J Am Oil Chem Soc 83(2):129–136

Snežana S-F, Milovan J, Olga B (2012) Epoxidation of castor oil with peracetic acid formed in situ in the presence of an ion exchange resin. Chem Eng Process 62:106–113

Soomro RA, Sherazi STH, Memon N, Shah MR, Kalwar NH, Hallam KR, Shah A (2014) Synthesis of air stable copper nanoparticles and their use in catalysis. Adv Mater Lett 5(4):191–198

Sui T, Song B, Zhang F, Yang Q (2016) Effects of functional groups on the tribological properties of hairy silica nanoparticles as an additive to polyalphaolefin. RSC Adv 6:393–402

Wäsche R, Hartelt M, Hodoroaba V-D (2015) Analysis of nanoscale wear particles from lubricated steel-steel contacts. Tribol Lett 58(49):1–10

Wei Y, Huaqing X (2012) A review on nanofluids: preparation, stability mechanism, and applications. J Nanomater 2012:1–17. https://doi.org/10.1155/2012/435873